DEVELOPMENTAL BIOLOGY 115, 490-501 (1986)

The Mechanisms and Mechanics of Archenteron Elongation during Sea Urchin Gastrulation

JEFFREY D. HARDIN* AND LOUIS Y. CHENG†

*Graduate Group in Biophysics and Medical Physics and †Department of Civil Engineering, University of California, Berkeley, California 94720

Received October 17, 1985; accepted in revised form January 10, 1986

Continued elongation of the archenteron during sea urchin gastrulation has long been thought to occur as a result of contraction of filopodia which are extended by secondary mesenchyme cells from the tip of the gut rudiment to the blastocoel roof. Here we present four lines of evidence which strongly suggest that forces generated within the archenteron itself can cause it to elongate. First, computer simulations based on the theory of solid mechanics show that filopodial pulling alone results in deformations not seen *in vivo*, and that observed shape changes can only be obtained by assuming that the archenteron is much less stiff than the rest of the embryo. Second, our transverse tissue sections of *Strongylocentrotus purpuratus* and similar sections of *Lytechinus pictus* reveal a marked decrease in the number of cells comprising the circumference of the archenteron during its elongation, demonstrating that the cells in the archenteron repack to form a longer, narrower array. Third, morphometric analysis of Nomarski DIC micrographs indicates no significant increase in the length/width ratios of cells in the archenteron due to filopodial pulling. Finally, *L. pictus* and *S. purpuratus* exogastrulae induced by treatment with 10 m*M* LiCl show complete gut extension accompanied by cell repacking without the action of secondary mesenchyme cells. These results strongly suggest that, in addition to any passive lengthening which may occur, the gut rudiment itself possesses an inherent capacity to elongate independent of filopodial pulling. On the basis of these findings, we propose that in at least some species, active cell rearrangement in the wall of the archenteron is the major contributing factor in the elongation of the gut rudiment, while the filopodia may primarily serve to guide the archenteron to the site of stomadeum formation.

INTRODUCTION

Gastrulation is a particularly striking morphogenetic process in many organisms. To understand the complex morphogenetic movements which occur during gastrulation, it is necessary not only to describe those movements, but also to investigate the forces which bring them about, since the shape of the embryo is a "diagram of forces" at work in the embryo (Thompson, 1961). One organism which has frequently been used to study such problems is the sea urchin. Sea urchin embryos are easily obtained in large numbers, they develop rapidly and synchronously, and many species are transparent, allowing detailed observation of cellular movements during morphogenesis.

Gastrulation in sea urchin embryos occurs in two phases (Dan and Okazaki, 1956; Gustafson and Kinnander, 1956). *Primary invagination* involves the inward buckling of the vegetal plate to form the archenteron (Figs. 1a, b). As primary invagination proceeds, the archenteron, which is roughly cylindrical in shape, extends $\frac{1}{4}$ to $\frac{1}{2}$ of the way across the blastocoel; the length of the gut rudiment varies depending on the species. A slight pause marks the end of primary invagination, during which time the archenteron does not appreciably increase in length (Gustafson and Kinnander, 1960).

The onset of *secondary invagination* is marked by the appearance of long, narrow filopodia on the basal surfaces of secondary mesenchyme cells at the tip of the gut rudiment (Figs. 1c, d). The filopodia continuously probe the inner surface of the blastocoel wall as gastrulation continues; those which make stable contacts with cells in the animal region form "cones of attachment," which appear to be portions of the basal lamina or the basal ends of ectoderm cells which are distended by the contracting filopodia (Kinnander and Gustafson, 1960). Elongation of the gut rudiment also resumes at approximately this time, and continues until the archenteron extends across the entire blastocoel (Figs. 1e, f). As the tip of the archenteron nears the blastocoel roof, it is apparently guided to the site of the oral primordium by filopodia which attach to the ectoderm in the future mouth region (Gustafson and Kinnander, 1960).

A number of workers have investigated the role of secondary mesenchyme cells during gastrulation in sea urchin embryos. The breakage or disappearance of filopodia either naturally (Gustafson and Wolpert, 1963) or following treatment of the embryos with low calcium,

0012-1606/86 $3.00

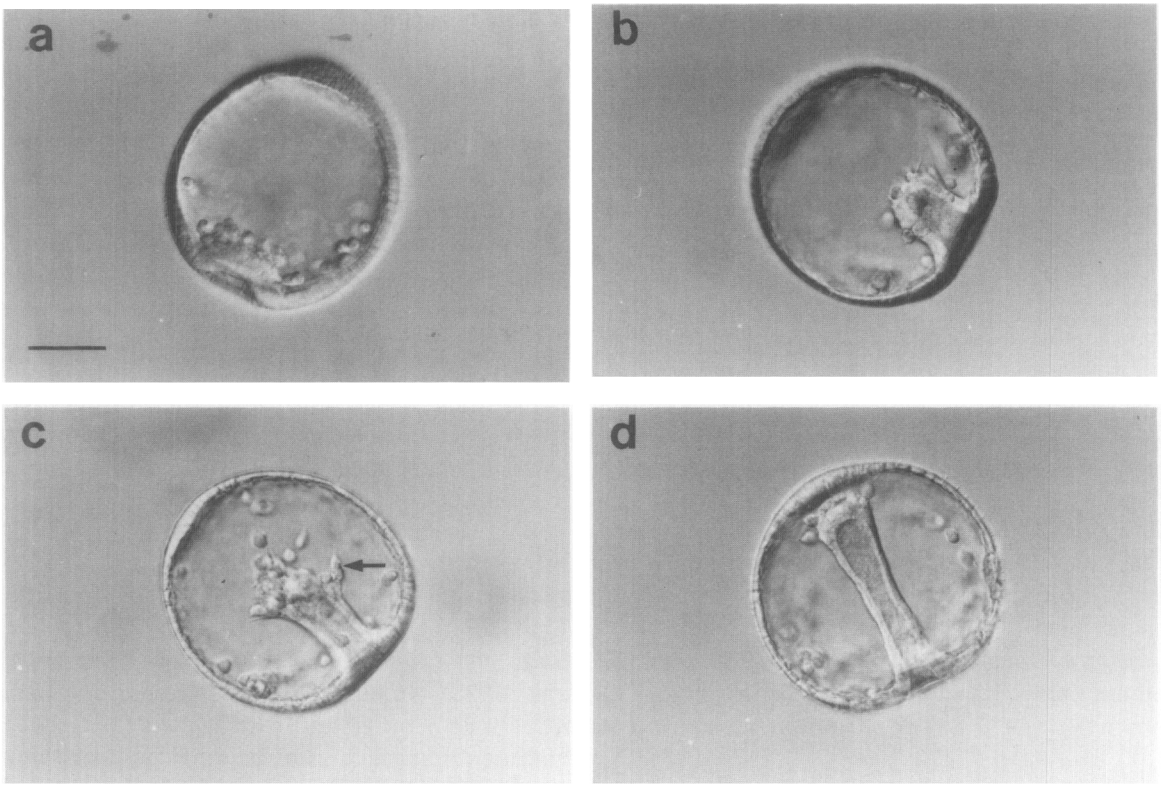

FIG. 1. Normal gastrulation in *Lytechinus pictus*. (a) Early gastrula. (b) Onset of secondary invagination. (c) Continuation of secondary invagination. Note the secondary mesenchyme cells at the tip of the archenteron (arrow). (d) Gastrulation completed. Bar = 50 μm.

pancreatin, or hypertonic sucrose (Dan and Okazaki, 1956), is correlated with failure of the archenteron to elongate fully. Colchicine and hydrostatic pressure disrupt microtubules in filopodia, and archenteron elongation ceases (Tilney and Gibbins, 1969). Lectins, such as concanavalin A, which appear to prevent the attachment of filopodia without interfering with their formation, also cause retraction of the archenteron (Spiegel and Burger, 1982).

These studies suggest that filopodia are important during sea urchin gastrulation. However, several questions remain unanswered. First, much of the current evidence for the filopodial contraction mechanism is circumstantial; treatments which disrupt filopodia may also affect other processes which are important in secondary invagination. Second, the precise *mechanical* role of filopodial contraction has not been clearly demonstrated, and remains poorly understood. In addition, there is evidence that secondary mesenchyme cells are not exclusively responsible for the lengthening of the archenteron. Although filopodial contraction may be important, it is not well coordinated with elongation of the gut rudiment in some species (Schroeder, 1981; Trinkaus, 1984). Furthermore, the phenomenon of exogastrulation suggests that the archenteron itself has at least some inherent capacity to elongate (Dan and Okazaki, 1956; Hörstadius, 1973). To clarify the processes at work during secondary invagination, we have used mechanical simulations, analysis of cell shapes, and the induction of abnormal gastrulation to investigate the cellular mechanisms and mechanics of archenteron elongation in two species of sea urchin, *Lytechinus pictus* and *Strongylocentrotus purpuratus*. Our studies strongly suggest that, in addition to whatever tension is generated by contracting filopodia, active forces exist which cause endodermal cells within the archenteron itself to rearrange to form a longer, narrower tube.

MATERIALS AND METHODS

Procurement of embryos. Gametes of *L. pictus* (Marinus, Pacific Biomarine) and *S. purpuratus* were obtained and fertilized as described by Hinegardner (1967). Fertilized eggs were placed in Millipore-filtered sea water (MPFSW) at a concentration of 0.25–0.5% and maintained at 16°C, either in large beakers with stirring paddles or in 6-ml aliquots in tissue culture dishes. Embryos were subsequently collected for experimental manipulation by gentle hand centrifugation.

Tissue sectioning. Embryos were collected and fixed in 1% glutaraldehyde in 90% MPFSW for 1 h (Ettensohn, 1984), and washed several times in phosphate-buffered

saline. Fixed and washed embryos were dehydrated in increasing concentrations of ethanol, cleared in Histosol (National Diagnostics), and embedded in Paraplast embedding medium (Monoject Scientific); embedded embryos were sectioned at a thickness of 10 μm. Sections were then stained with hematoxylin and eosin and examined using an Olympus differential interference contrast (DIC) microscope.

Microscopy. Embryos were attached to coverslips coated with a solution of 1 μg/ml poly-D-lysine HBr (Sigma), and mounted into one of two types of chamber for still photography and time-lapse videomicroscopy. Coverslips attached to the bottom of a shallow glass tissue culture dish were viewed with a Zeiss 40X water-immersion lens; coverslips attached to glass slides with dabs of silicone sealant or petroleum jelly were viewed with either a Zeiss 63X or Olympus 20X DIC lens. Chambers used for videomicroscopy were ringed with mineral oil to prevent evaporation while still allowing gas exchange to take place.

Morphometrics. Morphometric data were obtained using a Numonix model 1204 digitizer (Numonix Corp.) in conjunction with the MISYS morphometrics system (copyright C. M. Regen, 1982).

Exogastrulae. Exogastrulae were produced by treatment with LiCl according to a protocol slightly modified from Vacquier (1972). Embryos were transferred from normal sea water to 7.5–15 m*M* LiCl in MPFSW at the two-cell stage, and allowed to develop until the hatching blastula stage (*L. pictus*) or mesenchyme blastula stage (*S. purpuratus*), at which time the embryos were returned to normal sea water. Exogastrulae were then attached to coverslips and mounted in chambers for viewing.

RESULTS

Mechanical Simulations Show That Filopodial Pulling Alone Cannot Produce Observed Morphology

Proposals concerning the mechanics of the first phase of sea urchin gastrulation have a long history (e.g., Rhumbler, 1902; Moore and Burt, 1939; see Ettensohn, 1985b, for a review). However, secondary invagination has received comparatively little attention from a mechanical standpoint. To test the mechanical validity of the filopodial pulling mechanism, it would be desirable to stretch the archenteron artificially. However, since such direct testing is not feasible, mechanical modeling using the theory of solid mechanics provides a means for investigating the mechanical consequences of filopodial contraction for the shape of the embryo.

Mechanical modeling of analytically intractable problems in structural and bioengineering is usually carried out using the *finite element* method (Zienkiewicz, 1977; see Appendix); this method has proven useful in the mechanical modeling of a broad class of biological systems, including bone and connective tissues, such as arteries and lungs (Gallagher *et al.*, 1982). To apply finite element techniques to the sea urchin embryo, we have used a finite element program designed to analyze radially symmetric, or *axisymmetric*, thin-walled structures which undergo large deformations (Cheng, 1986; see Appendix). Such an axisymmetric model is an improvement over two-dimensional models of invagination (Odell *et al.*, 1981), since it accurately accounts for the three-dimensional nature of the system. In addition, these techniques have already proven useful in analyzing the deformations of sea urchin oocytes (Cheng, in preparation).

We present here the results of such modeling for two different, basic shapes, each of which is characteristic of a number of species of sea urchin. Figures 2a, b depict models of embryos such as *L. pictus*, *Mespilia globulus*, and *Clypleaster japonicus* (Dan and Okazaki, 1956; Okazaki, 1975), which are somewhat pear shaped, have relatively thin walls, and which have relatively short gut rudiments at the end of primary invagination. In contrast, Figs. 2c, d depict models of embryos such as *S. purpuratus*, *Pseudocentrotus depressus* (Okazaki, 1956), and *Psammechinus miliaris* (Gustafson and Kinnander,

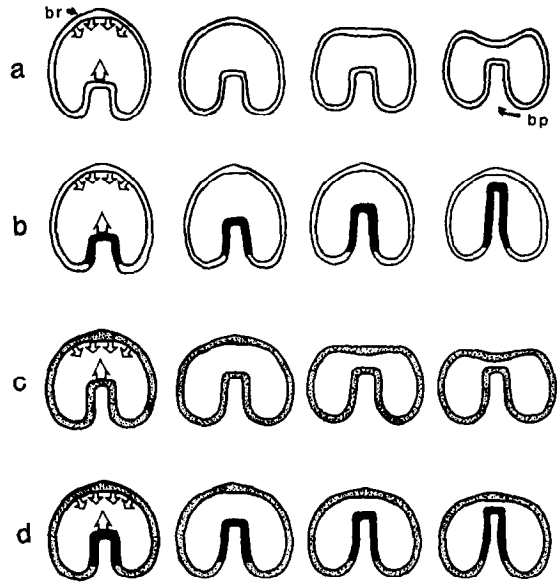

FIG. 2. Mechanical simulations of filopodial pulling. (a, b) Models of embryos such as *Lytechinus pictus*. (c, d) Models of embryos such as *Strongylocentrotus purpuratus*. In (a) and (c), the archenteron and surrounding ectoderm have the same mechanical properties. Note the extensive denting of the blastocoel roof (br). In (b) and (d), the archenteron is much more compliant than the rest of the embryo. Even in this case, the blastopore does not close (bp).

1956), which are more flattened, have somewhat thicker walls, and which have a relatively short distance to traverse during secondary invagination.

The first result of the mechanical simulations is that when such shapes are modeled as elastic structures solely under the influence of filopodial pulling, the correct morphology cannot be obtained (Figs. 2a, c). When the archenteron possesses the same mechanical properties as the rest of the embryo, denting of the roof of the blastocoel invariably results, especially in the case of *L. pictus* (Figs. 2a, c), but also in the case of *S. purpuratus*, though to a lesser extent. The noticeable thickening of the ectoderm at the animal pole does give this region a higher resistance to bending. When this difference in thickness is included in the model, however, it is not sufficient to prevent deflection of the blastocoel roof (Fig. 2). The intuitive reason for this denting effect is easy to see; when a cable exerts tension, it exerts the same amount of tension on either of its two ends. Thus if the filopodia generate enough tension to extend the archenteron, they must also exert an equivalent amount of tension on the blastocoel roof. When the shapes of actual embryos are compared with the predictions of the model, however, marked deflection of the blastocoel roof is never observed in the two species we have studied. An occasional *S. purpuratus* embryo will exhibit a small degree of denting, but *L. pictus* embryos have never been observed to undergo this type of deformation.

When the archenteron is assumed to be relatively more compliant than the rest of the embryo, the blastocoel roof does not deflect (Figs. 2b, d). In this case, less tension is required to distend the gut rudiment, and the relatively "stiff" ectoderm is able to withstand the traction exerted by the filopodia. Thus in order for the classical notion of filopodial traction to be consistent with the observed shape of the embryo, the archenteron wall must be much more compliant than the blastocoel roof.

However, even when the archenteron is assumed to be much more compliant than the rest of the embryo, two additional mechanical consequences of filopodial pulling are apparent. First, the blastopore does not constrict as the archenteron lengthens. This result is mechanically reasonable, since any further constriction of the blastopore would produce unfavorable bending stresses at the blastopore lip. *S. purpuratus* gastrulae do exhibit a relatively wide blastopore; however, the blastopores of *L. pictus* gastrulae show marked constriction (Fig. 3). Second, filopodial contraction results in a slight flattening of the embryo in the animal–vegetal direction. Here again, embryos such as *S. purpuratus* and *P. depressus* do exhibit some flattening; in contrast, embryos such as *L. pictus* maintain their pear-shaped structure (Fig. 3).

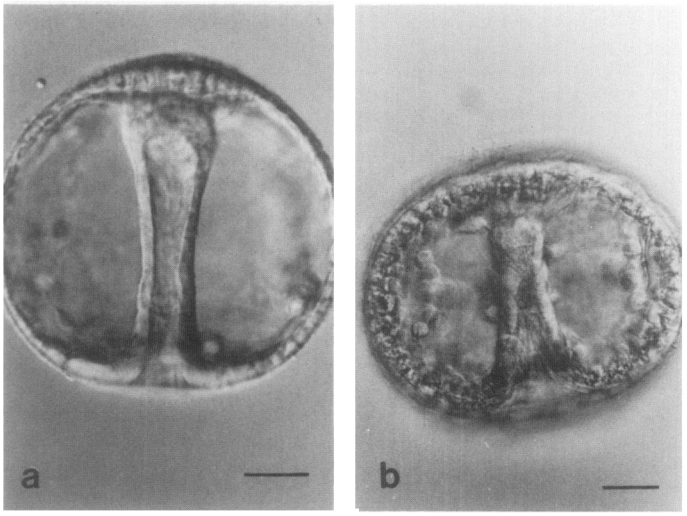

FIG. 3. Comparison of the shapes of *L. pictus* and *S. purpuratus* gastrulae. (a) *L. pictus*. (b) *S. purpuratus*. Bars = 25 μm.

In summary, these mechanical simulations suggest either that the blastocoel roof is very stiff relative to the archenteron or that filopodial traction plays a less prominent role in secondary invagination than was previously proposed. In the latter case, forces generated within the archenteron itself would also be important for its elongation.

Tissue Sections Show That Extensive Cell Rearrangements Occur in the Archenteron during Gastrulation

Many researchers have noted that the wall of the archenteron thins during gastrulation (Dan and Okazaki, 1956; Gustafson and Wolpert, 1963); however, changes in the dimensions of the archenteron have not been quantified. In addition, it is not known to what extent such changes contribute to secondary invagination, or how important other processes, such as active cell shape change and repacking, may be for archenteron elongation.

As Fristrom (1976) has pointed out, a cylindrical epithelial structure such as the archenteron can lengthen in one of two ways, assuming that no new material is added to the cylinder (Fig. 4). In Fig. 4a, individual cells increase in length without rearrangement to form a longer tube. Transverse sections through such a structure would not reveal a change in the number of cells in the circumference of the tube as it lengthens. In Fig. 4b, cells maintain their original dimensions, but they repack to form a longer cylinder with a smaller diameter. In this case, transverse sections would show a decrease in the number of cells in the circumference of the tube as it elongates.

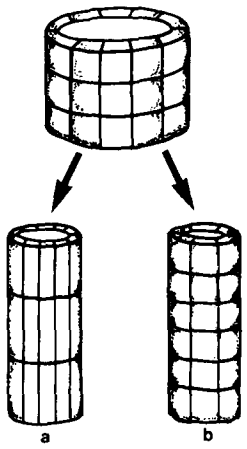

FIG. 4. Ways in which a cylindrical epithelial structure can elongate (after Fristrom, 1976). (a) Cells elongate without rearranging. In this case the number of cells in the circumference remains unchanged. (b) Cells repack without lengthening. In this case the number of cells in the circumference decreases.

To obtain information on both cell shape changes and cell repacking, we have analyzed transverse tissue sections of *L. pictus* and *S. purpuratus* gastrulae. When *L. pictus* and *S. purpurtatus* gastrulae are sectioned transversely at the mid- and late gastrula stages, two facts immediately emerge (Fig. 5). First, the wall of the archenteron thins markedly during gastrulation. The average decrease in thickness of cells in the wall of the archenteron is 34% for *S. purpuratus*, from 8.0 ± 0.1 μm to 5.3 ± 0.2 μm, while for *L. pictus* the decrease is 46%, from 15.2 ± 0.5 μm to 8.2 ± 0.3 μm (mean ± SE; Fig. 6). This thinning has been attributed to the passive stretching of the archenteron by filopodia (Dan and Okazaki, 1956). However, thinning could result from other mechanisms, including active cell shape changes (see below).

The second fact which becomes clear upon examining transverse sections of the archenteron is that a striking decrease in the number of cells in the circumference of the archenteron occurs during secondary invagination. Ettensohn (1985a) has shown this to be the case for *L. pictus*, and we have obtained similar results for *S. purpuratus* (Hardin and Cheng, 1985). When quantified, these results are even more striking. The average number of cells in the circumference of the gut rudiments of *S. purpuratus* gastrulae decreases by 41% from the mid- to late gastrula stages, from 16.0 ± 0.9 to 9.5 ± 0.3. The average decrease for *L. pictus* is more than 60%, from 18.5 ± 0.6 to 7.1 ± 0.3 (Fig. 7). It is unlikely that these decreases are due to cell death, since sagittal sections through the gut rudiment indicate that the total

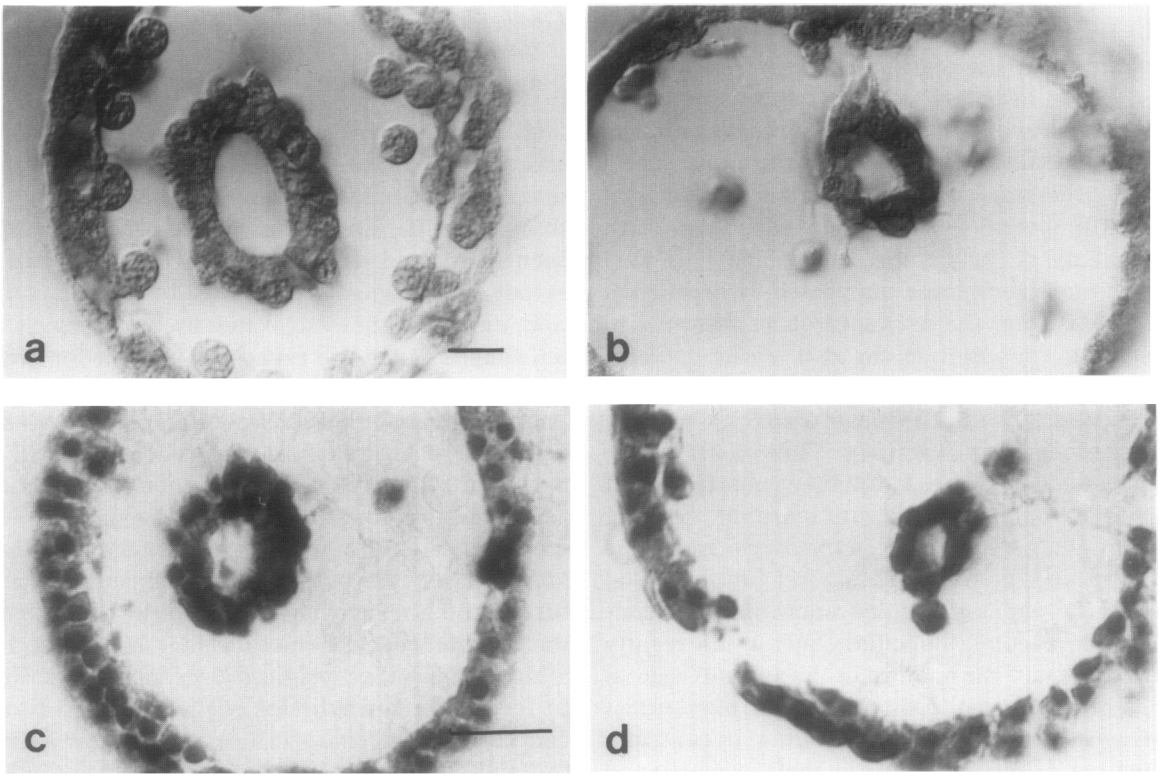

FIG. 5. Midtransverse paraffin sections of gastrulae at the beginning and end of secondary invagination. (a) *S. purpuratus* mid-gastrula. (b) *S. purpuratus* late gastrula. (c) *L. pictus* mid-gastrula. (d) *L. pictus* late gastrula. Bars = 10 μm.

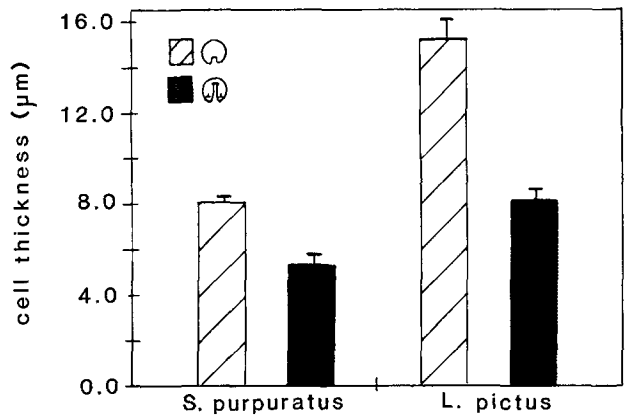

FIG. 6. Mean radial thickness (mean ± SE) of cells in the wall of the archenteron during secondary invagination for *S. purpuratus* and *L. pictus*. Measurements were made on mid-transverse paraffin sections for mid- (striped) and late (stippled) gastrulae.

number of cells in the archenteron does not decrease during secondary invagination. Instead, these decreases in cell number indicate that extensive cell repacking occurs during secondary invagination.

Cell Shapes in the Wall of the Archenteron Show That Cell Spreading Occurs during Secondary Invagination

The transparency of *L. pictus* embryos allows *in vivo* measurement of cell shapes in the wall of the archenteron using differential interference contrast (DIC) microscopy. Cell boundaries can be resolved if the embryo tightly adheres to a polylysine-coated coverslip in the proper orientation (Fig. 8). Tracings can then be made from video images or still photographs, and the length/width ratios of cells in the wall of the gut rudiment can be measured with the aid of a digitizer. Here "length" refers to projected length along the long axis of the gut

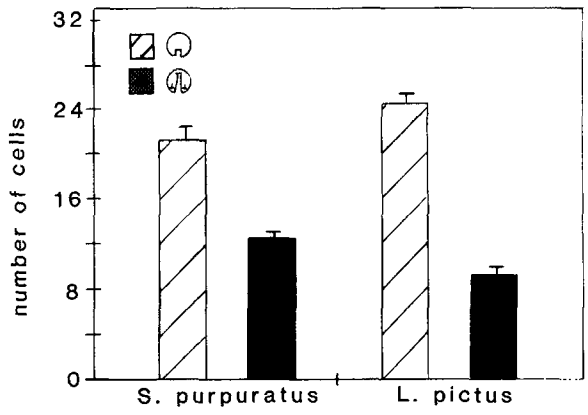

FIG. 7. Mean number of cells (mean ± SE) in the circumference of the archenteron during secondary invagination for *S. purpuratus* and *L. pictus*. Measurements were made on mid-transverse sections for mid- (striped) and late (stippled) gastrulae.

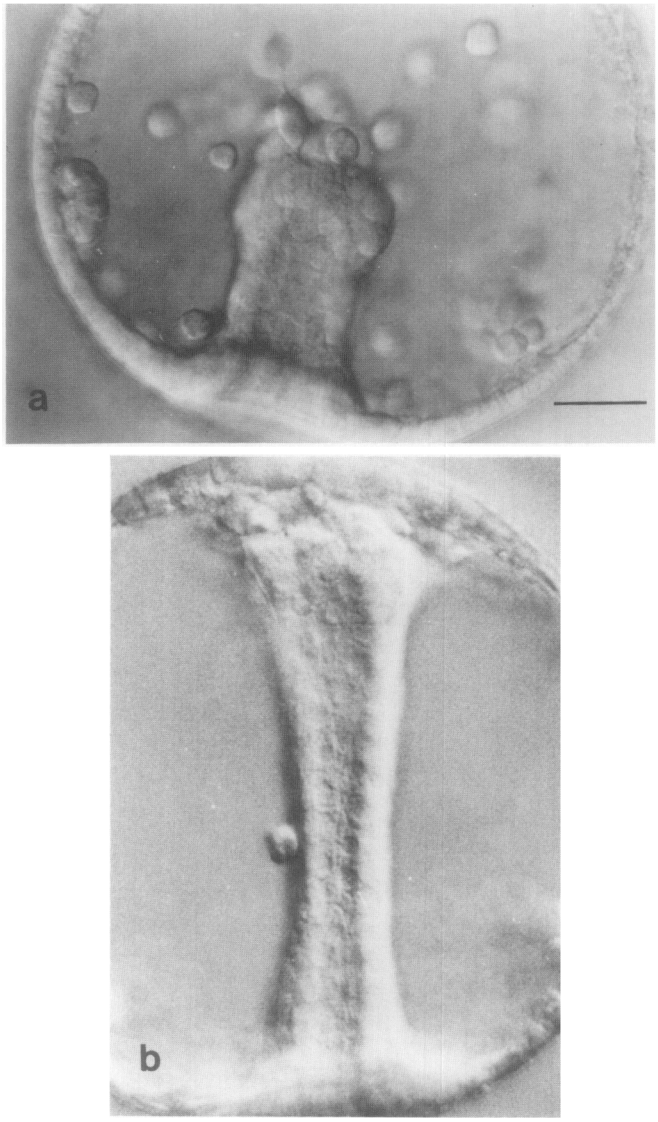

FIG. 8. Differential interference contrast micrographs of *L. pictus* gastrulae. (a) Mid-gastrula. (b) Late gastrula. Bar = 30 μm.

rudiment, while "width" refers to the projected length in the radial direction.

The results of such a procedure are shown in Fig. 9. The average length/width ratio of cells in the gut rudiments of midgastrula stage embryos is 1.08 ± 0.03 (mean ± SE). The average length/width ratio of cells in the archenterons of late gastrula stage embryos is 1.10 ± 0.03. This difference is not statistically significant at the 0.1 confidence level using a two-tailed Student's T test, and is quite consistent with the qualtitative results obtained by Ettensohn for *L. pictus* based on scanning electron microscopical observations (Ettensohn, 1985a). That no significant increase in the lengths of cells in the archenteron of *L. pictus* occurs during secondary invagination suggests that in this species thinning of the wall

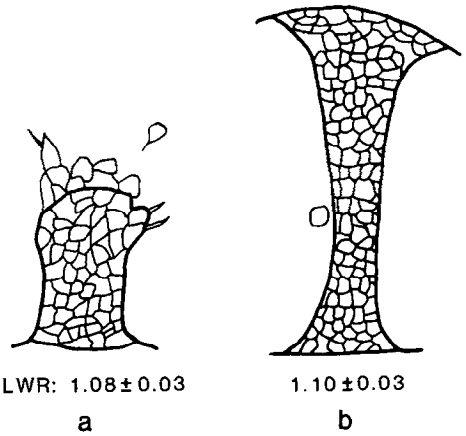

FIG. 9. Mean length/width ratios (mean ± SE) of cells in the wall of the archenteron during secondary invagination in *L. pictus*. "Length" refers to the projected length along the animal-vegetal axis, while "width" refers to the projected length in the radial direction.

of the gut rudiment is not primarily due to passive stretching.

Exogastrulation Shows That Full Extension of the Gut Rudiment Can Occur Without Filopodial Pulling

The artificial induction of exogastrulation in sea urchins was first described by Herbst (1893), who used the classic vegetalizing agent, lithium chloride. Since then, many other chemical agents have been found which can induce exogastrulation, including sodium azide (Child, 1948), low calcium (Okazaki, 1956), chloramphenicol (Hörstadius, 1963; Fujiwara and Yasumasu, 1974), and blastocoelic fluid components (Ishihara, Tonegawa, Suyemitsu, and Kubo, 1982). However, the effects of these different treatments vary widely, and as a result a great deal of confusion exists as to what constitutes "exogastrulation," as opposed to "vegetalization" (Gustafson and Wolpert, 1963). We reserve the term "exogastrula" for embryos which have everted gut rudiments, but exhibit otherwise normal morphology. "Normal" morphology would include proper proportions of endo- and ectoderm, the eventual proper partitioning of the gut rudiment into three regions, and the correct positioning and development of skeletal spicules. Embryos which possess disproportionately large amounts of endoderm are more properly referred to as "vegetalized."

The three most popular methods for producing exogastrulae have been low calcium (Okazaki, 1956; Amemiya *et al.*, 1979), chloramphenicol (Hörstadius, 1963; Fujiwara and Yasumasu, 1974; Mizoguchi and Yasumasu, 1983), and lithium chloride (Child, 1940; Vacquier, 1971). Low calcium treatment tends to result in shorter than normal gut rudiments, although these gut rudiments still possess the ability to differentiate into esophagus, stomach, and intestine (Amemiya *et al.*, 1979). Lithium chloride, and to some extent chloramphenicol, on the other hand, are capable of producing exogastrulae with full-length differentiated gut rudiments in some species. Lithium has proven particularly effective with *Dendraster excentricus* (Moore, 1927; Vacquier, 1971).

When precise doses of LiCl are administered for tightly controlled time periods, *L. pictus* embryos can also be induced to exogastrulate while maintaining otherwise normal morphology (Fig. 10). The process of evagination in such "full-length" exogastrulae appears to correspond closely to the invagination which normal gastrulae undergo. Exogastrulae with shorter gut rudiments produced by low calcium or shorter exposure to lithium begin the process of primary invagination apparently normally, and only later do their gut rudiments evert. Exogastrulae with full-length gut rudiments, on the other hand, undergo a direct evagination at the beginning of gastrulation (Fig. 10a). Time-lapse videomicroscopy reveals that the primary mesenchyme cells of such exogastrulae migrate out of the vegetal plate region after this "primary evagination" takes place, and eventually position themselves at the proper location to begin spicule formation (Fig. 10b).

Following the first phase of evagination, the gut rudiment lengthens in a manner similar to the normal process of secondary invagination (Fig. 10b). However, *elongation occurs without filopodial pulling by secondary mesenchyme cells.* Furthermore, secondary evagination is accompanied by a decrease in the number of cells around the circumference of the archenteron as in normal gastrulation. Although it was not possible to follow a single embryo throughout all of exogastrulation to ensure that the gut rudiment evaginated fully in every case, on the basis of counts made from DIC micrographs, the average number of cells decreases from 21 ± 1 to 13 ± 1 for *L. pictus* between early and mid- to late exogastrula stages (Fig. 11). Once this second phase of lengthening is complete, the gut rudiment differentiates, acquiring its characteristic tripartite structure (Fig. 10c). By this time the embryo has begun production of triradiate spicules; eventually an essentially normal, exogastrulated pluteus results (Fig. 10d). In addition to normal external morphology, LiCl-treated embryos have recently been shown to possess essentially normal septate junctions (Spiegel and Howard, 1985). Taken together, these results strongly suggest that the archenteron is not merely more compliant than the rest of the embryo, but that it actively elongates by cell arrangement.

When *S. purpuratus* embryos are treated with lithium chloride, they also exogastrulate. However, *S. purpuratus* exogastrulae usually have somewhat shortened gut rudiments, and appear similar to *Pseudocentrotus depressus* and *Hemicentrotus pulcherrimus* exogastrulae

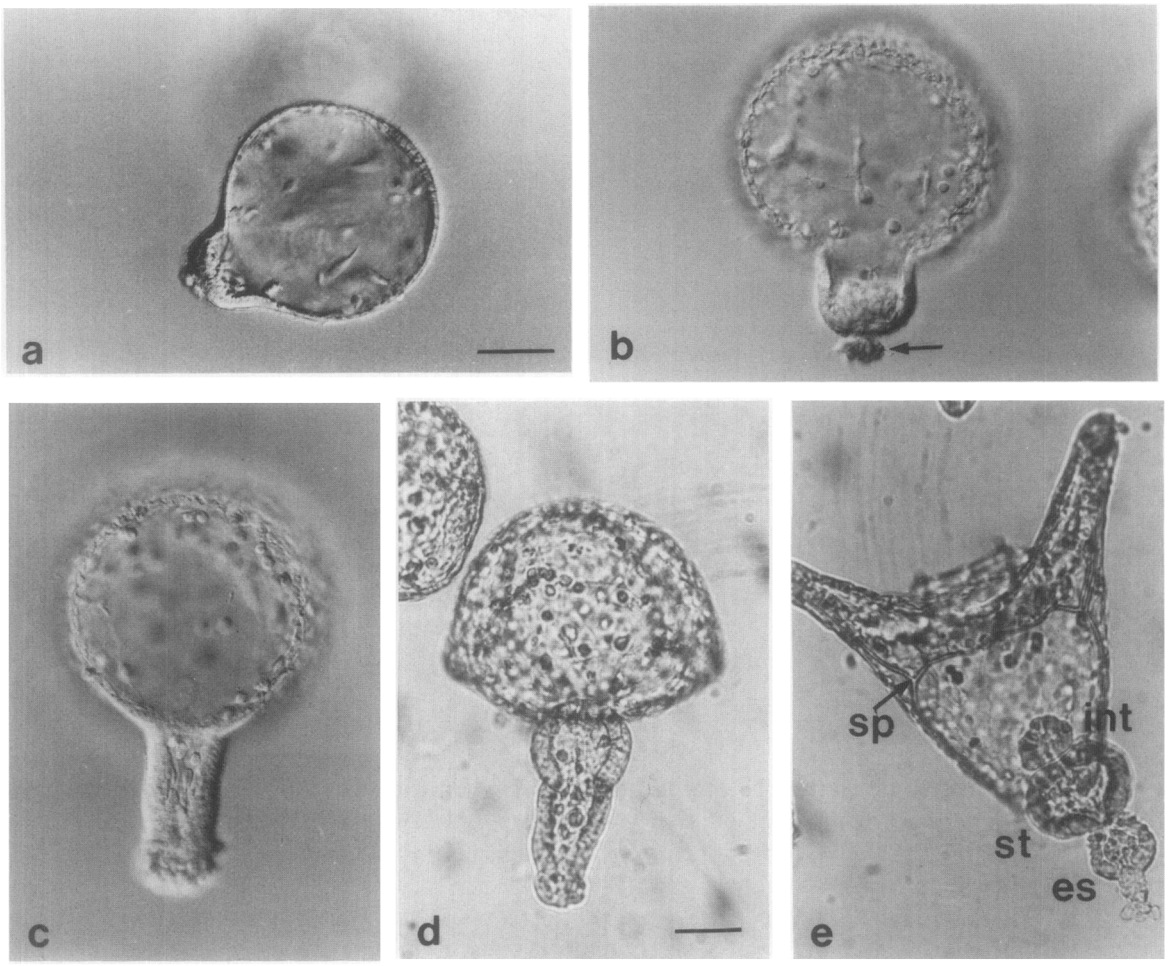

FIG. 10. LiCl-induced exogastrulation in *L. pictus*. (a) Early exogastrula. (b) Onset of secondary evagination. Mesenchymal cells are often extruded from the tip of the gut rudiment (arrow). (c) Mid-/late exogastrula. (d) Prism-stage exogastrula. (e) Pluteus-stage exogastrula. Note the normal development of skeletal spicules (sp), and the tripartite differentiation of the gut into esophagus (es), stomach (st), and intestine (int). Bar = 50 μm.

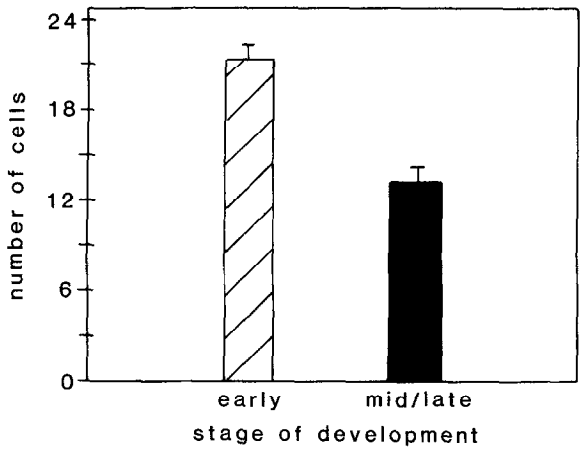

FIG. 11. Mean number of cells (mean ± SE) in the wall of the evaginated archenteron for early (striped) and mid-/late (stippled) *L. pictus* exogastrulae. Mean values were determined from superficial Nomarski DIC optical sections.

(Okazaki, 1956; Amemiya *et al.*, 1979). The gut rudiments of *S. purpuratus* exogastrulae also differentiate, and the embryos develop essentially normally (Fig. 12).

DISCUSSION

Filopodial pulling by secondary mesenchyme cells has traditionally been regarded as the sole mechanism responsible for secondary invagination during sea urchin gastrulation. Although it is clear that the filopodia generate tension (Gustafson, 1964), it is not clear that filopodial contraction is a *sufficient* mechanism for the elongation of the gut rudiment. Although it is true that treatments which disrupt filopodial formation and attachment (e.g., colchicine, lectins, inhibitors of collagen synthesis, and osmotic swelling) also interfere with gastrulation, in most cases it is possible and even probable that these treatments affect other processes occurring during secondary invagination. Similarly, although the

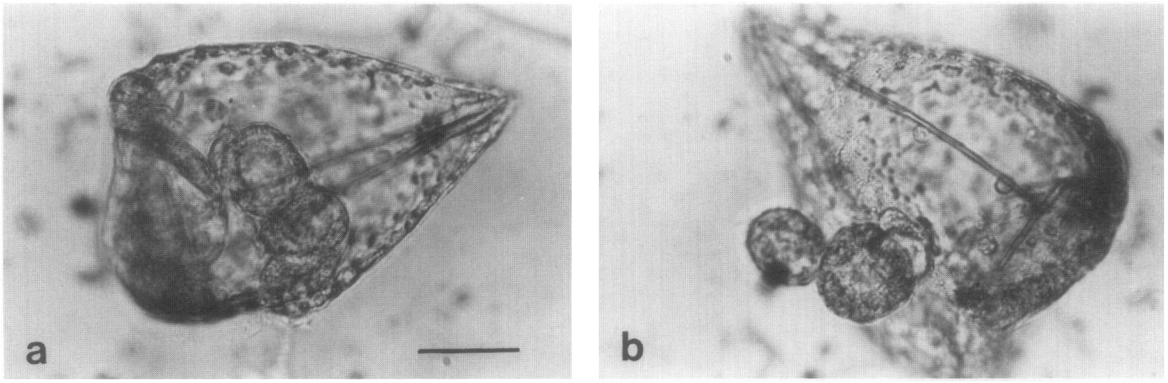

FIG. 12. LiCl-induced exogastrulation in *S. purpuratus*. (a) Normal early pluteus larva. (b) Exogastrulated early pluteus larva. Bar = 25 μm.

pause which separates primary and secondary invagination (Kinnander and Gustafson, 1960), can be correlated with the onset of the formation of filopodia, it may also signal the initiation of other processes at work during gastrulation.

If filopodial pulling is an important mechanism for lengthening the archenteron, then certain specific mechanical predictions can be made. First, denting of the blastocoel roof and flattening of the entire embryo will occur if the gut rudiment has the same mechanical properties as the rest of the embryo. In some species (e.g., *S. purpuratus* and *P. depressus*), some denting and flattening do appear to occur; in extreme cases, *P. depressus* embryos take on an almost "biconcave" appearance (Okazaki, 1956). Such flattening may represent an extreme response to filopodial traction. If no denting is to occur, the archenteron must be very compliant in comparison with the rest of the embryo, particularly in the case of species such as *L. pictus*. It is not known whether such a difference in mechanical properties actually exists in these embryos, although it is possible that cell repacking could contribute to the ability of the archenteron to undergo some passive stretching.

Second, filopodial pulling alone will produce a relatively wide blastopore. Indeed, the thicker-walled embryos we have examined tend to have wider blastopores (e.g., *S. purpuratus* and *P. depressus*). An extreme case of this type is the crinoid, *Comanthus japonica*, in which only a small space exists between the tip of the archenteron and the roof of the blastocoel, and in which the blastopore is extremely wide (Holland, 1978). However, embryos such as *L. pictus* and *Mespilia globulus* (Okazaki, 1975) possess constricted blastopores which actually decrease in diameter as gastrulation proceeds. In these species, some means of generating a circumferential constricting force seems to be necessary to close the blastopore.

Thinning of the wall of the gut rudiment had previously been ascribed to the passive stretching of the archenteron by contracting filopodia (Dan and Okazaki, 1956). However, thinning need not be solely due to stretching, but could result from active cell spreading, as is the case with some superficial cells during amphibian gastrulation (Keller, 1978). If stretching were the dominant mechanism, thinning would be accompanied by an increase in the lengths (along the animal-vegetal axis) of cells in the wall of the gut rudiment. If cells were to alter their shapes actively, however, an increase in the length-to-width ratio would not be required. In the case of *L. pictus*, little or no increase in length-width ratio occurs during secondary invagination, suggesting that active cell spreading is chiefly responsible for thinning of the gut rudiment in this species. As a result of this thinning, the total areas of both the inner and outer surfaces of the archenteron increase, which would partially offset the decrease in diameter due to cell rearrangement.

Tissue sections show that extensive cell rearrangements do occur in the gut rudiment during secondary invagination. The sharp decrease in the number of cells in the circumference of the archenteron during gastrulation indicates that the cells in the wall of the gut rudiment repack preferentially along the animal-vegetal axis to form a longer tube with smaller diameter. Further, the extent of rearrangement seems to be species dependent. For *L. pictus*, the nearly threefold decrease in circumferential cell number is nearly enough to account for the increase in length of the archenteron during secondary invagination. The extent of repacking in *S. purpuratus* is less, suggesting that cell rearrangement is less important in this species.

It could be argued that the cell rearrangements which are observed during gastrulation occur by a predominately passive mechanism (see above). However, the phenomenon of exogastrulation demonstrates that full extension of the gut rudiment can occur without filopodial pulling, strongly suggesting that active repacking of cells is involved in the normal process of elongation (Fig. 13). Further support for an autonomous extension mechanism comes from species which exhibit anomalous

secondary mesenchyme cell activity. In *Eucidaris tribuloides*, a "primitive" cidaroid urchin, no filopodia appear at the tip of the gut rudiment until it has invaginated quite deeply, and these filopodia do not appear to extend completely across the blastocoel (Schroeder, 1981). In *Lytechinus variegatus*, filopodia are initially extended laterally and even in the vegetal direction; only later in gastrulation do they make contact with the blastocoel roof (Trinkaus, 1984; Morrill and Santos, 1985).

In addition, it is interesting to note that it is considerably easier to induce *L. pictus* exogastrulae with full-length gut rudiments than it is to induce a similar response in *S. purpuratus*. While this difference may simply reflect differing sensitivities to lithium chloride, in conjunction with mechanical and cell rearrangement data these observations suggest that both filopodial pulling and autonomous cell rearrangement contribute to secondary invagination. The relative contributions which the two processes make seem to vary among different species, which could account for the wide range of morphologies observed among different sea urchin embryos.

Sources of new material which might also increase the length of the archenteron seem to be relatively unimportant during secondary invagination. Vital dye fate mapping in *Paracentrotus lividus* (Hörstadius, 1973), local application of vital dye in *L. pictus* gastrulae, and measurements of total cellular volume in the archenteron of early and late *L. pictus* gastrulae (J. Hardin, unpublished observations) indicate that few cells roll over the blastopore lip during secondary invagination. Moreover, only 10-20% of the cells in the embryo, including the archenteron, appear to undergo division during this time (Agrell, 1953; Hinegardner, 1967; Takahashi and Okazaki, 1979; Burke, 1980; J. Hardin, unpublished observations), and it is unlikely that cell growth accompanies those cell divisions which do occur, since feeding does not begin until the pluteus stage. That gastrulation occurs despite the inhibition of DNA synthesis and subsequent cytokinesis using the DNA polymerase α inhibitor, aphidicolin, indicates that mitosis is unnecessary for gastrulation to occur (Stephens *et al.*, 1986).

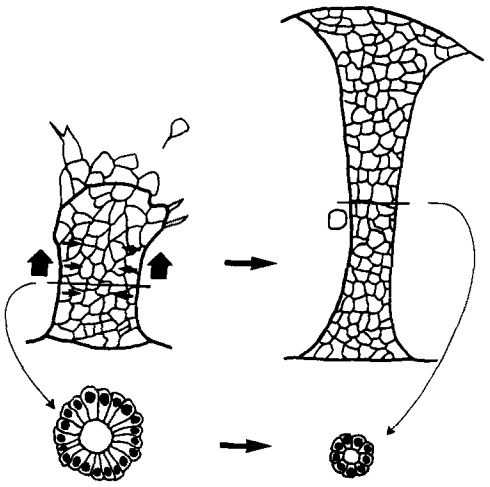

FIG. 13. A model for the role of active cell repacking in archenteron elongation. Convergence of cells radially toward the axis of the archenteron causes it to elongate, with a concomitant decrease in the number of cells in the circumference.

While autonomous cell rearrangement appears to be an important mechanism for archenteron elongation, filopodia are nevertheless important for the proper completion of gastrulation for several reasons. First, filopodia probably lend lateral stability to the lengthening gut rudiment. Certain treatments which disrupt collagen crosslinking do not seem to prevent elongation of the archenteron in *S. purpuratus* and *L. pictus*, but the gut rudiment remains flaccid (Butler, Hardin, and Benson, 1986, in preparation), suggesting that filopodia stabilize the gut rudiment in an upright position. Second, filopodia guide the archenteron to the site of the future mouth. In *P. miliaris*, for example, filopodia are sent out laterally to the stomadeal region once the gut rudiment has elongated (Gustafson and Kinnander, 1960). Also, the stomodeal region possesses distinct antigenic markers prior to contact by filopodia (Coffman *et al.*, 1985), suggesting that the filopodia may recognize specific cell surface markers in the future mouth area.

It is not currently known how a monolayered epithelium such as the sea urchin archenteron undergoes cell rearrangement, although recent evidence suggests that lamellipodial activity of the basal surfaces of endoderm cells coupled with subsequent cell shape changes may be involved (Hardin and Benson, 1986, in preparation). In the two cases in which epithelial cell rearrangement has been observed directly, in the dorsal marginal zone of *Xenopus* gastrulae (Keller, 1981) and at the margin of the enveloping layer during teleost epiboly (Keller and Trinkaus, 1982), rearranging cells appear to move past one another without any obvious protrusive activity (R. E. Keller, personal communication). Moreover, epithelial cell rearrangement can apparently take place despite the presence of septate or tight junctions. This has been demonstrated by the use of transmission electron microscopy for two species of sea urchin (Spiegel and Howard, 1983; Ettensohn, 1985a), as well as during evagination of imaginal discs in *Drosophila* (Fristrom, 1982) and teleost epiboly (Kageyama, 1982). It seems clear that as cells rearrange they must break and reform junctional contacts; models for such junctional rearrangement have been proposed (Fristrom, 1982; Jacobson *et al.*, 1986). In addition, the kinetics of junction formation may place limits on the speed with which such rearrangements occur. Although little information is

available regarding such processes, vertebrate tight junctions may be able to form within a few minutes (Hudspeth, 1982; Regen and Steinhardt, 1986). In any event, however, such models of junctional rearrangement say nothing about the forces generated by the cells themselves which allow them to repack. This more fundamental question must be answered if the mechanics of epithelial cell rearrangement in general, and sea urchin gastrulation in particular, are to be understood.

We thank G. Oster and C. Ettensohn for their many helpful comments on the manuscript, and R. Keller and F. Wilt for their suggestions and encouragement during the course of the research. This work was supported by an NSF predoctoral fellowship to J. Hardin, NIH Grant HD15403 to F. Wilt, NSF Grant PCM8110985 and NIH Grant HD18979-01A1 to R. Keller, and NSF Grant MCS10557 to G. Oster.

APPENDIX: THE FINITE ELEMENT METHOD AND AXISYMMETRIC SHELL ANALYSIS

We use a simplified but illustrative approach here to describe the mechanical modeling of filopodial contraction in sea urchin embryos. Readers interested in the technical development of the method are referred to Zienkiewicz (1977) for the finite element method, and Cheng (1986) for the axisymmetric shell element used in this study.

The finite element method is based on a variational formulation which minimizes a functional representing the total energy of the system. A material body is first divided into a collection of subbodies; each subbody is modeled by a *finite element* which represents its geometric and mechanical characteristics. The method then computes the contributions to the energy functional from all of the elements, and minimizes the total to obtain the solution of the problem. Because no restrictions are placed on the shapes and physical properties of the elements, problems involving complicated geometries and regions with differing mechanical properties may be analyzed using this method.

Formulating the energy functional of the system requires the consideration of three kinds of relationships: the *equilibrium equations*, which equate the external forces (pulling by the filopodia in this case) with the stresses; the *kinematic relations*, which relate the strains within the material to the displacements, and the *constitutive relations*, which relate stresses to strains. In the case of thin-walled, axisymmetric structures such as the sea urchin embryo, the general three-dimensional theory of solid mechanics can be specialized to account for the thinness of the shell.

First, the equilibrium equations in terms of stresses, valid for large deformations, are integrated over the thickness of the shell. The resulting shell equilibrium equations are expressed in terms of *stress resultants*, comprised of membrane and shear forces and bending moments. It should be emphasized that these forces and moments have components both in the plane of symmetry, as well as in the "hoop" direction, so that the axisymmetry of the body is accounted for. Second, the thinness of the shell allows the kinematic assumption to be made that *plane sections remain plane*, and possibly rotated, when deformation takes place. The strains calculated within the shell are based on this assumption. Finally, Hooke's law is also specialized for the shell to relate the stress resultants and the strains. The resulting theory is capable of modeling finite stretching, shearing, and bending of the shell.

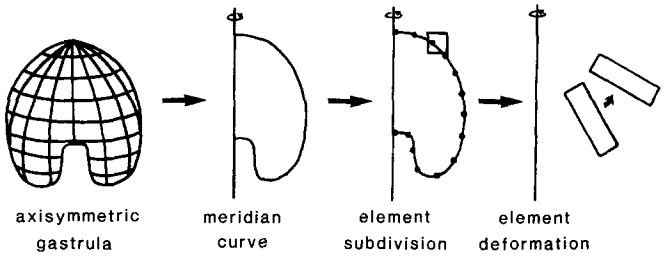

FIG. A1. The finite element modeling process applied to sea urchin gastrulation.

The modeling process for a typical embryo is schematically represented in Fig. A1. The geometry of the embryo is *axisymmetric*, and it remains so throughout secondary invagination for the species we are modeling. Thus the motion of a *meridian curve* lying in the plane of symmetry fully characterizes the deformation pattern for this three-dimensional, thin-walled body. This meridian curve represents the *continuum model* of the embryo. In the *finite element model*, the meridian curve is modeled by 50 shell elements joined end-to-end. Loads simulating the action of filopodial pulling are then imposed on the finite element model, and the deformation pattern of the model embryo is determined.

REFERENCES

AGRELL, I. (1953). A mitotic gradient in the sea urchin embryo during gastrulation. *Arch. Zool.* **6**, 213–217.

AMEMIYA, S., AKASAKA, K., and TERAYAMA, H. (1979). Reversal of polarity in ciliated cells of the isolated sea urchin pluteus gut. *J. Exp. Zool.* **210**, 177–182.

BURKE, R. D. (1980). Morphogenesis of the digestive tract of the pluteus larva of *Strongylocentrotus purpuratus:* Shaping and bending. *Int. J. Invert. Reprod.* **2**, 13–21.

CHENG, L. Y. (1986). Applications of mechanics to cell and developmental biology. Report #UCB/SESM 86/01, Dept. Civil Engin., Univ. Calif., Berkeley.

CHILD, C. M. (1940). Lithium and echinoderm gastrulation: With a review of the physiological-gradient concept. *Physiol. Zool.* **13**, 4–41.

CHILD, C. M. (1948). Exogastrulation by sodium azide and other inhibiting conditions in *Strongylocentrotus purpuratus. J. Exp. Zool.* **107**, 1–38.

COFFMAN, J., NELSON, S., and MCCLAY, D. R. (1985). A cell surface protein that identifies the ventral surface of the ectoderm of sea urchin gastrulae. *J. Cell Biol.* **101**, 469a.

DAN, K., and OKAZAKI, K. (1956). Cyto-embryological studies of sea

urchins. III. Role of the secondary mesenchyme cells in the formation of the primitive gut in sea urchin larvae. *Biol. Bull.* **110,** 29-42.

ETTENSOHN, C. A. (1984). Primary invagination of the vegetal plate during sea urchin gastrulation. *Amer. Zool.* **24,** 571-588.

ETTENSOHN, C. A. (1985a). Gastrulation in the sea urchin embryo is accompanied by the rearrangement of invaginating epithelial cells. *Dev. Biol.* **112,** 383-390.

ETTENSOHN, C. A. (1985b). Mechanisms of epithelial invagination. *Quart. Rev. Biol.* **60,** 289-307.

FRISTROM, D. (1976). The mechanism of evagination of imaginal disks of *Drosophila*. III. Evidence for cell rearrangement. *Dev. Biol.* **54,** 163-171.

FRISTROM, D. K. (1982). Septate junctions in imaginal disks of Drosophila: A model for the redistribution of septa during cell rearrangement. *J. Cell. Biol.* **94,** 77-87.

FUJIWARA, A., and YASUMASU, I. (1974). Some observations of abnormal embryos induced by short-period treatment with chloramphenicol during early development of sea urchin. *Dev. Growth Differ.* **16,** 83-92.

GALLAGHER, R. H., SIMON, B. R., JOHNSON, P. C., and GROSS, J. F., ed. (1982). "Finite Elements in Biomechanics." Wiley, N.Y.

GUSTAFSON, T. (1964). The role and activities of pseudopodia during morphogenesis of the sea urchin larva. *In* "Primitive Motile Systems" (R. D. Allen and N. Kamiya, eds.), pp. 333-350. Academic Press, Orlando, Fla.

GUSTAFSON, T., and KINNANDER, H. (1956). Microaquaria for time-lapse cinematographic studies of morphogenesis in swimming larvae and observations on gastrulation. *Exp. Cell Res.* **11,** 36-57.

GUSTAFSON, T., and KINNANDER, H. (1960). Cellular mechanisms in morphogenesis of the sea urchin gastrula. The oral contact. *Exp. Cell Res.* **21,** 361-373.

GUSTAFSON, T., and WOLPERT, L. (1963). The cellular basis of morphogenesis and sea urchin development. *Int. Rev. Cytol.* **15,** 139-214.

HARDIN, J., and CHENG, L. (1985). Mechanisms of archenteron elongation during sea urchin gastrulation. *J. Cell Biol.* **101,** 92a.

HERBST, C. (1893). Experimentelle Untersuchungen über den Einfluss der veränderten Mediums auf die Entwickelung der Thiere. I. Theil. Versuche an Seeigeleiern. *Zeitschr. Wiss. Zool.* **55,** 446-518.

HINEGARDNER, R. (1967). Echinoderms. *In* "Methods in Developmental Biology" (F. H. Wilt and N. K. Wessels, eds.), pp. 130-155. Thomas Y. Crowell, New York.

HOLLAND, N. D. (1978). The fine structure of *Comanthus japonica* (Echinodermata: Crinoidea) from zygote through early gastrula. *Tissue Cell* **10,** 93-112.

HÖRSTADIUS, S. (1963). Vegetalization of sea urchin larvae by chloramphenicol. *Dev. Biol.* **7,** 144-151.

HÖRSTADIUS, S. (1973). "Experimental Embryology of Echinoderms." Clarendon Press, Oxford.

HUDSPETH, A. J. (1982). The recovery of local transepithelial resistance following single-cell lesions. *Exp. Cell Res.* **138,** 331-342.

ISHIHARA, K., TONEGAWA, Y., SUYEMITSU, T., and KUBO, K. (1982). The blastocoelic fluid of sea urchin embryo induces exogastrulation. *J. Exp. Zool.* **220,** 227-233.

JACOBSON, A. G., ODELL, G. M., OSTER, G. F., and CHENG, L. Y. (1986). Neurulation and the cortical tractor model for epithelial folding. *J. Embr. Exp. Morph.*, in press.

KAGEYAMA, T. (1982). Cellular basis of epiboly of the enveloping layer in the embryo of the medaka, *Oryzias latipes*. II. Evidence for cell rearrangement. *J. Exp. Zool.* **219,** 241-256.

KELLER, R. E. (1978). Time-lapse cinematographic analysis of superficial cell behavior during and prior to gastrulation in *Xenopus laevis*. *J. Morphol.* **157,** 223-248.

KELLER, R. E. (1981). An experimental analysis of the role of bottle cells and the deep marginal zone in gastrulation of *Xenopus laevis*. *J. Exp. Zool.* **216,** 81-101.

KELLER, R., and TRINKAUS, J. P. (1982). Cell rearrangement in a tightly joined epithelial layer during *Fundulus* epiboly. *J. Cell Biol.* **95,** 325a.

KINNANDER, H., and GUSTAFSON, T. (1960). Further studies on the cellular basis of gastrulation in the sea urchin larva. *Exp. Cell Res.* **19,** 276-290.

MIZOGUCHI, H., and YASUMASU, I. (1983). Effect of α,α'-dipyridyl on exogut formation in vegetalized embryos of the sea urchin. *Dev. Growth Differ.* **25,** 57-64.

MOORE, A. R. (1927). Self differentiation of intestine in larvae of sand urchin, *Dendraster eccentricus*. *Proc. Soc. Exp. Biol. Med.* **25,** 40-41.

MOORE, A. R., and BURT, A. S. (1939). On the locus and nature of the forces causing gastrulation in the embryos of *Dendraster excentricus*. *J. Exp. Zool.* **82,** 159-171.

MORRILL, J. B., and SANTOS, L. L. (1985). A scanning electron microscopical overview of cellular and extracellular patterns during blastulation and gastrulation in the sea urchin, *Lytechinus variegatus*. *In* "The Cellular and Molecular Biology of Invertebrate Development" (R. H. Sawyer and R. M. Showman, eds.), Univ. South Carolina Press, Columbia, S.C., pp. 3-33.

ODELL, G. M., OSTER, G., ALBERCH, P., and BURNSIDE, B. (1981). The mechanical basis of morphogenesis. I. Epithelial folding and invagination. *Dev. Biol.* **85,** 446-462.

OKAZAKI, K. (1956). Exogastrulation induced by calcium deficiency in the sea urchin, *Pseudocentrotus depressus*. *Embryologia* **3,** 23-36.

OKAZAKI, K. (1975). Normal development to metamorphosis. *In* "The Sea Urchin Embryo" (G. Czikak, ed.), pp. 177-232. Springer-Verlag, Berlin.

REGEN, C. M., and STEINHARDT, R. A. (1986). Global properties of the *Xenopus* blastula are mediated by a high resistance epithelial seal. *Dev. Biol.* **113,** 147-154.

RHUMBLER, L. (1902). Zur Mechanik des Gastrulationvorganges insbesondere der Invagination. *Wilhelm Rouxs Arch. Entwicklungsmech.* **14,** 401-476.

SCHROEDER, T. (1981). Development of a "primitive" sea urchin (*Eucidaris tribuloides*): irregularities in the hyaline layer, micromeres, and primary mesenchyme. *Biol. Bull.* **161,** 141-151.

SPIEGEL, E., and HOWARD, L. (1983). Development of cell junctions in sea urchin embryos. *J. Cell Sci.* **62,** 27-48.

SPIEGEL, E., and HOWARD, L. (1985). The coincident time-space patterns of septate junction development in normal and exogastrulated sea urchin embryos. *Exp. Cell Res.* **161,** 75-87.

SPIEGEL, M., and BURGER, M. M. (1982). Cell adhesion during gastrulation: A new approach. *Exp. Cell Res.* **139,** 377-382.

STEPHENS, L., HARDIN, J., KELLER, R., and WILT, F. (1986). The effects of aphidicolin on morphogenesis and differentiation in the sea urchin embryo. Submitted for publication.

TAKAHASHI, M. M., and OKAZAKI, K. (1979). Total cell number and number of the primary mesenchyme cells in whole, $\frac{1}{2}$ and $\frac{1}{4}$ larvae of *Clypleaster japonicus*. *Dev. Growth Differ.* **21,** 553-566.

THOMPSON, D. W. (1961). "On Growth and Form," abridged edition (J. T. Bonner, ed.), Cambridge Univ. Press, Cambridge.

TILNEY, L. G., and GIBBINS, J. R. (1969). Microtubules and filaments in the filopodia of the secondary mesenchyme cells of *Arbacia punctulata* and *Echinarachnius parma*. *J. Cell Sci.* **5,** 195-210.

TRINKAUS, J. P. (1984). "Cells Into Organs: The Forces That Shape the Embryo," 2nd ed. Prentice-Hall, Englewood Cliffs.

VACQUIER, V. D. (1971). The effects of glucose and lithium chloride on the appearance of β-1,3-glucanohydrase activity in sand dollar plutei. *Dev. Biol.* **26,** 11-16.

ZIENKIEWICZ, O. C. (1977). "The Finite Element Method" 3rd ed. McGraw-Hill, London.